

Published in final edited form as:

Sci Signal. ; 5(253): ra89. doi:10.1126/scisignal.2003264.

G Protein–Coupled Receptor–Mediated Activation of p110 β by G $\beta\gamma$ Is Required for Cellular Transformation and Invasiveness

Hashem A. Dbouk^{1,*}, Oscar Vadas^{2,*}, Aliaksei Shymanets³, John E. Burke², Rachel S. Salamon¹, Bassem D. Khalil¹, Mathew O. Barrett⁴, Gary L. Waldo⁴, Chinmay Surve⁵, Christine Hsueh⁶, Olga Perisic², Christian Harteneck³, Peter R. Shepherd⁷, T. Kendall Harden⁴, Alan V. Smrcka⁵, Ronald Taussig⁸, Anne R. Bresnick⁶, Bernd Nürnberg³, Roger L. Williams^{2,†}, and Jonathan M. Backer^{1,†}

¹Department of Molecular Pharmacology, Albert Einstein College of Medicine, Bronx, NY, 10461, USA ²MRC Laboratory of Molecular Biology, Cambridge, CB2 0QH, UK ³Department of Pharmacology and Experimental Therapy, Institute for Pharmacology and Toxicology and Interfaculty Center of Pharmacogenomics and Pharma Research Eberhard-Karls-Universität Tübingen, Tübingen, 72074, Germany ⁴Department of Pharmacology, University of North Carolina School of Medicine, Chapel Hill, NC 27599, USA ⁵Department of Pharmacology and Physiology, University of Rochester School of Medicine and Dentistry, Rochester, NY 14642, USA ⁶Department of Biochemistry, Albert Einstein College of Medicine, Bronx, NY, 10461, USA ⁷Department of Molecular Medicine and Pathology, University of Auckland, New Zealand ⁸Department of Pharmacology, University of Texas Southwestern Medical Center, Dallas, TX 75390, USA

Abstract

Synergistic activation by heterotrimeric guanine nucleotide–binding protein (G protein)–coupled receptors (GPCRs) and receptor tyrosine kinases distinguishes p110 β from other class IA phosphoinositide 3-kinases (PI3Ks). Activation of p110 β is specifically implicated in various physiological and pathophysiological processes, such as the growth of tumors deficient in phosphatase and tensin homolog deleted from chromosome 10 (PTEN). To determine the specific

[†]To whom correspondence should be addressed: rlw@mrc-lmb.cam.ac.uk (R.L.W.) or jonathan.backer@einstein.yu.edu (J.M.B.).

*These authors contributed equally to this work.

Author contributions: H.A.D. identified the potential G $\beta\gamma$ interaction site by sequence analysis, produced mutants, analyzed mutant construct activity, performed cell culture analysis of p110 β mutants, conducted peptide inhibition experiments for signaling, Boyden chamber and proliferation assays, prepared figures, and contributed to writing the paper. O.V. identified the potential G $\beta\gamma$ interaction site by HDX-MS, produced and purified PI3K mutants for in vitro activity assays and HDX-MS, carried out in vitro kinase assays, analyzed mutant construct activity, carried out all of the HDX-MS experiments, prepared figures, and contributed to writing the paper. A.S. expressed and purified proteins, including all of the G $\beta\gamma$ that was used for the HDX-MS, and conducted assays on recombinant p85/p110 β . J.E.B. contributed to HDX-MS experiments and data analysis, and helped revise the manuscript. R.S.S. analyzed p110 β binding to Rab5. B.D.K. conducted Boyden chamber experiments. M.O.B. performed cell-based PLC β experiments. G.L.W. performed in vitro PLC β experiments. C.S. performed binding experiments with peptides and G $\beta\gamma$ subunits. C.Hsueh performed collagen invasion assays. O.P. contributed to cloning, expression, purification, and activity assays of p110 β constructs, and helped revise the manuscript. C.Harteneck contributed to expression, purification, and activity assays of G $\beta\gamma$ and PI3-kinases. P.R.S. supervised the synthesis of the PI3K inhibitors. T.K.H. supervised the PLC β experiments and provided purified G $\beta\gamma$. A.V.S. supervised binding experiments with peptides and G $\beta\gamma$ subunits. R.T. conducted the adenylyl cyclase assays. A.R.B. contributed to the design and analysis of chemotaxis assays. B.N. provided purified G $\beta\gamma$ for kinase assays and HDX-MS experiments, and contributed to the design and analysis of assays on peptide and G $\beta\gamma$ effects on p110 β activity of various PI3K β constructs, and contributed to writing of the manuscript. R.L.W. contributed to the design and analysis of the HDX-MS experiments and the p110 β mutagenesis experiments, and contributed to writing the manuscript. J.M.B. contributed to the design and analysis of the p110 β mutagenesis and the p110 β activity and signaling experiments, and contributed to writing the manuscript.

Competing interests: H.A.D., R.S.S., B.D.K., and J.M.B. have a patent pending on the development of therapeutics targeting the p110 β -G $\beta\gamma$ interface. P.R.S. is a founder scientist of Pathway Therapeutics.

contribution of GPCR signaling to p110 β -dependent functions, we identified the site in p110 β that binds to the G $\beta\gamma$ subunit of G proteins. Mutation of this site eliminated G $\beta\gamma$ -dependent activation of PI3K β (a dimer of p110 β and the p85 regulatory subunit) in vitro and in cells, without affecting basal activity or phosphotyrosine peptide-mediated activation. Disrupting the p110 β -G $\beta\gamma$ interaction by mutation or with a cell-permeable peptide inhibitor blocked the transforming capacity of PI3K β in fibroblasts, and reduced proliferation, chemotaxis, and invasiveness of PTEN-null tumor cells in culture. Our data suggest that specifically targeting GPCR signaling to PI3K β could provide a therapeutic approach for tumors that depend on p110 β for growth and metastasis.

Introduction

Signaling by class I phosphoinositide 3-kinases (PI3Ks) is commonly enhanced in tumors by gene amplification, activating mutations, or the inactivation of phosphatase and tensin homolog deleted from chromosome 10 (PTEN), a tumor suppressor lipid phosphatase [1]. Class I PI3Ks produce phosphatidylinositol-3,4,5-trisphosphate (PIP₃) in cells and stimulate proliferation, survival, and motility. The class IA enzymes are obligate heterodimers consisting of distinct catalytic (p110) subunits bound to the same regulatory (p85) subunits [2, 3]. Among the three class IA PI3Ks, the *PIK3CB* gene product p110 β is unique, because it can be activated both by receptor tyrosine kinases (RTKs) and downstream of heterotrimeric guanine nucleotide-binding protein (G protein)-coupled receptors (GPCRs) through direct binding to G $\beta\gamma$ subunits [4–7]. PTEN-deficient prostate cancer development specifically depends on the activity of the p110 β -p85 dimer (referred to as PI3 K β), but the mechanism for this specificity is currently unknown [8–11]. Whether GPCRs have a role in PI3K β -mediated transformation of PTEN-null cells has remained an open question because of the lack of tools to specifically probe the G $\beta\gamma$ -PI3K β interaction.

Defining the role of G $\beta\gamma$ in activating effectors such as p110 β is challenging because of the transient nature of interactions between the two and because of the lack of a distinct G $\beta\gamma$ -binding motif that could be used to identify its target binding sites. This contrasts with the mechanism of activation of PI3Ks by RTKs, which involves high-affinity interactions that have been well characterized [12, 13]. To investigate the mechanism of p110 β activation downstream of GPCRs by G $\beta\gamma$, and to define the role of this interaction in p110 β signaling in cells, we have identified the G $\beta\gamma$ -binding site on p110 β . We took two parallel approaches, the first based on an analysis of sequence conservation, and the second with hydrogen-deuterium exchange mass spectrometry (HDX-MS). Both approaches identified the same region, enabling us to generate a p110 β mutant that remained sensitive to stimulation by RTKs but did not respond to activation by G $\beta\gamma$. This mutant enabled us to interrogate the physiological importance of p110 β activation downstream of GPCRs by G $\beta\gamma$, and to define a critical role for this interaction in the cellular transformation, proliferation, and chemotaxis of PTEN -null tumor cells.

Results

Identification of the G $\beta\gamma$ -binding site in p110 β

We previously showed that the adaptor-binding, Ras-binding, and C2 domains of p110 β are not responsible for its activation by G $\beta\gamma$ subunits [14]. For this reason, we compared the remainder of the p110 β sequence with those of p110 α and p110 δ , which are insensitive to stimulation by G $\beta\gamma$, to look for sequence differences that might account for the selective activation of p110 β by G $\beta\gamma$. Whereas the helical and kinase domains of all three isoforms display high sequence similarity, we identified a 24-amino acid residue, non-conserved region (residues 514 to 537) in the linker between the C2 domain and the helical domain of

p110 β (Fig. 1A and fig. S1). The central portion of this segment is not visible in the crystal structure of p110 β , presumably because it is disordered, but it is part of a surface-accessible loop [15].

In parallel, we used an empirical approach, HDX-MS, to experimentally identify the p110 β -G $\beta\gamma$ interaction sites. HDX-MS is a powerful technique to monitor protein dynamics, protein-protein interactions, as well as protein-lipid interactions [16–19]. For HDX-MS measurements, we used two experimental setups, one with soluble G $\beta\gamma$ (G γ -C68S) (Fig. 1, B and C), and another with lipid-modified G $\beta\gamma$ in the presence of membranes (fig. S2). To enhance the stability of interaction between the p110 β -p85 dimer and soluble G $\beta\gamma$ in solution, we produced a heterotrimer containing p110 β , G γ C68S, and a chimeric construct containing G β covalently linked to a fragment of p85 α containing the C-terminal Src homology 2 (SH2) domain and the coiled-coil domain (iSH2-cSH2) (Fig. 1B). This heterotrimer formed a stable complex that could be stimulated by both a platelet-derived growth factor receptor (PDGFR)-derived bis-phosphopeptide (pY) and G $\beta_1\gamma_2$ subunits (G $\beta\gamma$) (fig. S3A). When we compared differences in the hydrogen-deuterium (HD) exchange rates of p110 β peptides between the heterotrimeric fusion complex and the wild-type p110 β -p85 α -icSH2 heterodimer, we identified two stretches that were more protected in the fusion complex (Fig. 1C and fig. S3, B and C). The first potential G $\beta\gamma$ -binding site, containing residues 518 to 538, matched very well with the region mapped by sequence analysis. The second protected region, amino acids 557 to 578, lies underneath the C2-helical linker. Changes in this region are likely a result of indirect effects from the binding of G $\beta\gamma$ to the linker above it. The same regions of p110 β binding to G $\beta\gamma$ were identified with full-length PI3K β and lipidated G $\beta\gamma$, with liposomes to stabilize the interactions (fig. S2, C and D, tables S1 to S6). Taken together, the sequence analysis and HDX-MS data suggested that the region of p110 β spanning residues 518 to 537 was the G $\beta\gamma$ -binding site.

To test whether this region was involved in G $\beta\gamma$ -mediated regulation of p110 β , we designed a loop-swap p110 β mutant in which these 24 amino acid residues were replaced with the corresponding region of p110 δ (Fig. 1D). We also mutated residues lysines 532 and 533 (⁵³²KK) in the p110 β loop, which are highly conserved among p110 β from different species but not between p110 β and p110 α or p110 δ , and which are ordered in the p110 β crystal structure (Fig. 1E) [20]. Replacement of the p110 β loop with that of p110 δ or mutation of ⁵³²KK to DD had no effect on the *in vitro* basal kinase activity of PI3K β in assays with purified enzyme from insect cells (Fig. 1F) or in assays with enzyme immunopurified from mammalian cells (fig. S4, A and B). However, whereas wild-type PI3K β was markedly activated by the addition of G $\beta\gamma$, neither the ⁵³²KK-DD mutant nor the loop-swap mutant of PI3K β was activated by G $\beta\gamma$ (Fig. 1F, figs. S4 A and B). Wild-type and mutant enzymes were activated to a similar extent by pY (Fig. 1F, S4A, S4B), even though the mutation sits close to the predicted p85-nSH2-binding site (Fig. 1C) [21]. Similar results were obtained with a ⁵¹⁴KAAEI-DAAKA mutant of p110 β , which targets the N-terminal end of the loop (fig. S4C). The degree of activation of PI3K β by pY and G $\beta\gamma$ (Fig. 1) was consistent with previous studies with baculovirally-expressed PI3K β purified from insect cells [7, 15], although it was substantially greater than that seen with PI3K β immunopurified from transfected mammalian cells (fig. S4). These differences in fold activation may reflect the influences of assay conditions (see the Supplementary Materials), N-terminal tags on basal activity, or the presence of an antibody bound to the immunopurified enzyme [2, 22].

Role of G $\beta\gamma$ -mediated activation of p110 β in signaling, transformation, and cell motility

To measure the effect of the p110 β mutation on signaling to the serine and threonine kinase Akt, we transfected human embryonic kidney (HEK) 293E cells with plasmids encoding the wild-type or ⁵³²KK-DD mutant p110 β together with plasmids encoding p85 α and myc-tagged Akt (myc-Akt), with or without plasmids encoding G $\beta_1\gamma_2$ subunits, which activate

p110 β in vitro [23]. G $\beta\gamma$ -dependent Akt activation in this system was specifically inhibited by the p110 β inhibitor TGX-221, and therefore reflected G $\beta\gamma$ -mediated stimulation of p110 β (fig. S5A). Whereas cells containing wild-type PI3K β showed a marked increase in the abundance of Akt activated by phosphorylation at Thr³⁰⁸ (pT308-Akt) in the presence of exogenous G $\beta\gamma$ subunits, cells transfected with plasmid encoding the ⁵³²KK-DD mutant PI3K β showed a complete loss of Akt activation in the presence of G $\beta\gamma$ subunits (Fig. 2A). Similarly, lysophosphatidic acid (LPA)-stimulated Akt activation was greater in NIH3T3 cells stably expressing wild-type PI3K β than in cells expressing the ⁵³²KK-DD mutant p100 β (Fig. 2B). The ⁵³²KK-DD mutation had no effect on the binding of p110 β to the small guanosine triphosphatase (GTPase) Rab5 (Fig. 2C), indicating that interactions of mutant p110 β with other intracellular regulators were intact. These data show that the C2-helical linker region of p110 β is necessary for G $\beta\gamma$ -mediated activation of PI3K β in vitro and in cells.

To test the biological relevance of G $\beta\gamma$ -mediated activation in p110 β signaling, we compared the ability of wild-type and mutant p110 β constructs to mediate cellular transformation and motility. In a soft agar colony formation assay, cells transfected with plasmid encoding wild-type PI3K β generated substantially more colonies than did control cells. However, transfection of cells with plasmid encoding the ⁵³²KK-DD mutant PI3K β resulted in a complete loss of transformation (Fig. 2D, fig. S5B). Similar results were obtained in a focus formation assay, in which NIH3T3 cells transfected with plasmid encoding wild-type PI3K β formed a substantially greater number of foci compared to that formed by cells transfected with plasmid encoding the ⁵³²KK-DD mutant PI3K β (Fig. 2E, fig. S5C). This result was not because of differences in proliferation, because wild-type and mutant p110 β caused similar increases in proliferation as compared to that of control NIH 3T3 cells (fig. S6A). Similarly, wild-type, but not mutant, p110 β increased the extent of chemotaxis of cells toward serum in a Boyden chamber assay (Fig. 2F). The ability of wild-type p110 β to enhance transformation and migration was G $\beta\gamma$ -dependent, because it was inhibited by pertussis toxin (fig. S6, B and C). These data showed that GPCR inputs to PI3K β , transmitted by G $\beta\gamma$, are critical for PI3K β -mediated cellular transformation and enhancement of motility.

Identification of the p110 β -binding site on G $\beta\gamma$ by HDX-MS

To explore the possibility of specifically inhibiting the interactions between p110 β and G $\beta\gamma$, we used the HDX-MS approach to determine the region on G $\beta\gamma$ that binds to p110 β (Fig. 3). We identified two regions on G $\beta\gamma$ that were more protected in the fusion compared to in the free G $\beta\gamma$. One of the peptides spans residues 31 to 45 in G β , in the linker between the N-terminal α -helix and the first blade of the β -propeller (Fig. 3, A and B). This region was not previously observed to interact with other G $\beta\gamma$ effectors. The other more protected stretch spans residues 85 to 99 in the second blade of the β -propeller, a region previously identified to be of major importance for the activation of phospholipase C β 2 (PLC- β 2) [24, 25]. This region contains the residue Trp⁹⁹ at the top of the propeller, which is part of the “hot-spot” region in G β that makes contacts with several effectors [26]. These data showed that p110 β shares a common G $\beta\gamma$ -binding surface with other effectors, such as the G protein α -subunit (Fig. 3C), PLC- β , adenylyl cyclase [27], and PI3K γ [28], but that it also uniquely affects a linker region between the N-terminal α -helix and the first blade of G β . This interface could provide an attractive target for therapeutics, because targeted disruption of this interface should have relatively specific effects on G $\beta\gamma$ -mediated activation of p110 β .

Inhibition of the proliferation, chemotaxis and invasion of PTEN-null tumor cells by a peptide inhibitor of the p110 β -G $\beta\gamma$ interaction

To generate an inhibitor of p110 β -G $\beta\gamma$ interactions, we synthesized a peptide derived from the C2-helical linker region of p110 β (⁵¹⁴KAAEIASSDSANVSSRGGKKFLPV). The peptide had no effect on basal PI3K β activity (Fig. 4A), but blocked G $\beta\gamma$ -dependent activation of PI3K β in vitro, whereas a scrambled peptide had no effect (Fig. 4B). Similar results were obtained with N-myristoylated and N-TAT-labeled versions of the peptide (Fig. 4C), which are cell-permeable versions of the peptide. The peptide had no effect on G $\beta\gamma$ -mediated activation of p101–p110 γ dimers, which were inhibited by peptides that target the canonical G $\beta\gamma$ effector-binding site (SIGK and QEHA, Fig. 4D).

We tested the effects of the myristoylated peptide on G $\beta\gamma$ -mediated activation of Akt in NIH3T3 cells transfected with plasmid encoding myc-Akt with or without plasmids encoding G $\beta\gamma$ subunits. The myristoylated p110 β -peptide completely inhibited G $\beta\gamma$ -mediated (Fig. 5A) and LPA-stimulated (Fig. 5B) increases in Akt phosphorylation at Thr³⁰⁸ at a concentration of 30 μ M (fig. S7A), whereas myristoylated scrambled peptide or vehicle control had minimal effects. In contrast, the myristoylated peptide had no effect on epidermal growth factor (EGF)-dependent activation of Akt in a cell line in which TGX221 had a substantial inhibitory effect (fig. S7B), which showed that the myristoylated peptide had no effect on RTK-mediated activation of PI3K β in intact cells. The inhibitory activity of the myristoylated peptide required its entry into the cells, because both myristoylated and TAT-tagged peptides inhibited G $\beta\gamma$ -dependent activation of Akt, whereas unlabeled peptide had no such effect (fig. S7C). In addition, the myristoylated p110 β -peptide, but not the myristoylated scrambled peptide, inhibited PI3K β -dependent transformation of NIH3T3 cells, as was observed in a soft agar colony formation assays (Fig. 5C and fig. S5B) and focus formation assays (Fig. 5D and fig. S5C). Inhibition of cellular transformation by the myristoylated p110 β -peptide was not a result of decreased proliferation, because neither the myristoylated peptide nor pertussis toxin inhibited the proliferation of NIH3T3 cells transfected with plasmid encoding PI3K β (fig. S7D). In contrast, the myristoylated peptide had no effect on cellular transformation caused by expression of oncogenic Ras (Fig. 5E). The myristoylated peptide also blocked the enhanced migration in a Boyden chamber assay of NIH3T3 cells transfected with plasmid encoding PI3K β (fig. S5F).

Control experiments showed that the effects of the myristoylated peptide were specific for p110 β -G $\beta\gamma$ interactions. The myristoylated peptide did not reduce the abundance of p110 β protein (Fig. 5, C and D). In addition, the myristoylated p110 β peptide had no effect on G $\beta\gamma$ -dependent activation of the class IB PI3K (the p101–p110 γ dimer) (fig. S8A), the synergistic activation of adenylyl cyclase by G $\beta\gamma$ and G α_s (fig. S8B), or the G $\beta\gamma$ -mediated activation of PLC- β in cells (fig. S8, C), and the non-modified peptide had no effect on G $\beta\gamma$ -mediated activation of PLC- β in vitro (fig. S8, D). Similarly, the myristoylated peptide had no effect on the binding of p110 β to Rab5 or on the p110 β -dependent induction of autophagy (fig. S8, E and F) [29], which is in agreement with the ⁵³²KK-DD mutant p110 β having no effect on Rab5 binding (Fig. 2C). Thus, the effects of the myristoylated peptide specifically disrupted p110 β -G $\beta\gamma$ interactions. These data showed that p110 β -mediated cellular transformation and migration requires the binding of p110 β to G $\beta\gamma$.

The growth of PTEN-null tumors depends on p110 β [8], and inhibition of G $\beta\gamma$ signaling or knock-in of a kinase-deficient p110 β blocks the growth of prostate cancer cells [9, 30]. To test the role of p110 β -G $\beta\gamma$ interactions in PTEN-null prostate cancer cells, we measured the proliferation of PC3 cells in the presence of myristoylated p110 β -peptide or scrambled peptide. Whereas PC3 cell proliferation was unaffected by the myristoylated scrambled peptide or by the p110 β inhibitor TGX221, proliferation was inhibited in the presence of myristoylated p110 β -peptide or pertussis toxin (Fig. 6A). Similar effects were seen in the

PTEN-null endometrial cancer cell lines AN3CA and RL95-2, but not in the PTEN-replete endometrial cancer line KLE (Fig. 6B). Myristoylated p110 β -peptide also inhibited the chemotaxis of PC3 cells toward serum in a Boyden chamber assay (Fig. 6C). Finally, in a collagen invasion assay designed to mimic paracrine interactions between macrophages and tumor cells during invasion [31], macrophage-dependent PC3 cell invasion was blocked by the myristoylated p110 β -peptide (Fig. 6D), but not by myristoylated scrambled peptide. These data suggest that GPCR-mediated activation of p110 β in PTEN-null cells plays a critical role in proliferation, chemotaxis, and in paracrine interactions between tumor cells and macrophages during invasion.

Discussion

Over the last few years, there has been an increased appreciation of the roles of GPCRs in cancer, both through direct signaling and by transactivation of RTKs [32–34]. Although the activation of the PI3K β isoform of PI3K by G $\beta\gamma$ subunits has been known for many years, the mechanism of this interaction is unclear, and it has been difficult to specifically study GPCR-regulated signaling by PI3K β . Our identification of the G $\beta\gamma$ -binding site in p110 β , and the reciprocal p110 β -binding site in G $\beta\gamma$, has enabled the construction of mutants and peptide-based inhibitors that specifically disrupt this interaction. Using these approaches, we have demonstrated a critical role for G $\beta\gamma$ signaling to PI3K β in p110 β -mediated transformation, as well as in the proliferation and invasion of PTEN-null prostate cancer cells. Our data suggest that GPCR-mediated activation of PI3K β could provide a new target for the design of anticancer therapeutics.

The G $\beta\gamma$ -binding site comprises a surface loop that bridges helices L α 5 and H1A between the C2 and helical domains of p110 β . This loop is close to the inhibitory contact site for the nSH2 domain of p85 (Glu⁵⁵²). We can propose two mechanisms for the activation of p110 β by G $\beta\gamma$: one through membrane recruitment, and the other through relief of SH2-mediated inhibition. These mechanisms are not mutually exclusive, and it is likely that both contribute. G $\beta\gamma$ stimulates p110 β in the absence of p85 [7], as well as when p110 β was associated with a p85 construct consisting of only the iSH2 domain (p85-i) or with a construct possessing the iSH2 connected to the inhibitory cSH2 domain (p85-ic) (fig. S9). Furthermore, G $\beta\gamma$ activated PI3K β in the absence of pY (Fig. 1F). Consequently, relief of SH2-mediated inhibition cannot be the only mechanism of activation of p110 β by G $\beta\gamma$. Our studies with PI3K β and G $\beta\gamma$ in the presence of liposomes showed that G $\beta\gamma$ -binding enhanced interactions of the kinase domain with lipid membranes (fig. S2, B and D). This suggests that a portion of the activation mechanism involves increased targeting to membranes because of the lipid moiety of the prenylated G $\beta\gamma$. On the other hand, activation of p110 β by pY peptides involves the relief of inhibition by the N- and C-terminal SH2 domains [15], and both pY and G $\beta\gamma$ are required for maximal stimulation of PI3K β . It is possible that pY binding to the nSH2 only partially relieves its inhibitory contact, and that G $\beta\gamma$ more completely displaces it to achieve full activation. It is also possible that by G $\beta\gamma$ increasing the membrane affinity, the presence of the membrane surface sterically helps to displace the inhibitory N- and C-terminal SH2 domains. Of note, the G $\beta\gamma$ -binding region of p110 β shows low sequence similarity with the corresponding region of the other G $\beta\gamma$ -regulated PI3K catalytic subunit, p110 γ . Consequently, it is not straightforward to predict the G $\beta\gamma$ -binding region of p110 γ , and this will require experimental mapping.

Because the peptide inhibitor did not affect the activity of p110 β directly, we presume that its mechanism of action is through binding to the p110 β -interacting site within G $\beta\gamma$. HDX-MS analysis of p110 β binding to G $\beta\gamma$ revealed a partial overlap with surfaces that bind to canonical G $\beta\gamma$ effectors, as well as a region that appears to be unique to p110 β : the linker region between the N-terminal α -helix and the first blade of G β . We have not determined the

binding site for the p110 β -derived peptide within G $\beta\gamma$. However, the specificity of the peptide's effects for the interaction between G $\beta\gamma$ and p110 β , rather than to adenylyl cyclase, PLC- β or p101-p110 γ , suggests that the peptide interacts with the unique region of the p110 β -binding surface in G $\beta\gamma$. An alternative explanation accommodates the fact that the binding of p110 β to G $\beta\gamma$ is weak relative to that of other canonical effectors. In this model, the p110 β peptide may bind to a portion of the canonical interface, but with an affinity low enough to displace p110 β , but not other G $\beta\gamma$ effectors. We cannot experimentally distinguish between these hypotheses at this time. Finally, it is formally possible that the peptide contacts G $\beta\gamma$ in a manner that is distinct from that which occurs with the corresponding loop in p110 β . Studies are in progress to define the peptide-binding site, and these will be useful in designing a better inhibitor of the G $\beta\gamma$ -p110 β interaction.

PI3K β is ubiquitously-expressed and has been implicated in the regulation of vascular tone [35], thrombogenesis [36], male fertility [37], phagocytosis in macrophages [38], and integrin signaling [39]. In addition, p110 β has kinase-independent functions, including involvement in clathrin-mediated endocytosis, cell proliferation, and DNA repair [10, 40, 41]. The role of GPCR signaling to PI3K β in these systems can now be directly addressed. With regard to the requirement for PI3K β in PTEN-null tumors [8], our data suggest that G $\beta\gamma$ interactions with PI3K β are critical for the growth and invasion of these tumors. Surprisingly, the peptide was more efficacious in inhibiting the proliferation of PC3 cells than was the p110 β -specific kinase inhibitor TGX221. This is consistent with studies showing that kinase-deficient p110 β rescues proliferative defects in mice [10, 40], and suggests that at least some of the G $\beta\gamma$ signaling to p110 β involves the scaffolding functions of p110 β . In contrast, previous studies have shown that kinase-deficient p110 β does not support transformation in PTEN-null cells [8], suggesting that stimulation of PI3K β activity by G $\beta\gamma$ is required for transformation.

The role of GPCR signaling in PTEN-null tumors has not been extensively studied. It will be important to determine whether peptidomimetics or other small-molecule inhibitors of the p110 β -G $\beta\gamma$ interface might be therapeutically useful in the treatment of some PTEN-null tumors. Currently, we do not know which GPCRs function upstream of G $\beta\gamma$ in the activation, targeting, or both of PI3K β . Defining these upstream inputs would provide an alternative approach to the treatment of tumors dependent on p110 β .

Materials and Methods

Design and cloning of constructs and transfections

The ⁵³²KK-DD mutant was generated with the Quick-change kit (Stratagene). The G β -p85 α -icSH2 fusion construct was cloned with standard digestion and ligation strategies, linking the sequence encoding the C-terminus of human G β 1 to that encoding the N-terminus of human p85 α -ic (residues 432 to 724) with a 25-residue linker of the following sequence: GSPGISGGGGPGSGGGGSGGGGSG. All mutants were confirmed by sequencing. Transfections were performed with Fugene HD (Roche).

Purification of p110 β -p85 α dimers expressed in insect cells

Recombinant baculoviruses were generated and propagated with the Bac-to-Bac expression system (Invitrogen) according to the manufacturer's recommendations. For expression, 3 L of *Spodoptera frugiperda* (Sf9) cells at a density of 1.0×10^6 cells/ml were co-infected with an optimized ratio of viruses encoding complexes of the catalytic and regulatory subunit of PI3K. After 55 hours of infection at 27°C, cells were harvested and washed with ice-cold phosphate-buffered saline (PBS) supplemented with 0.5 mM 4-(2-Aminoethyl) benzenesulfonyl fluoride hydrochloride (AEBSF; (Melford). Subsequently, cells were lysed

by sonication for 4 min in 120 ml of buffer A1 [20 mM Tris (pH 8), 300 mM NaCl, 10 mM imidazole] containing 0.5 mM AEBSF, and were centrifuged for 20 min at 140,000g. The supernatant was filtered through a 0.45- μ m Minisart filter unit (Sartorius Biotech) before loading onto two connected 5-ml HisTrap FF columns (GE Healthcare). The columns were washed first with buffer A1 and then with buffer A2 [20 mM Tris (pH 8), 100 mM NaCl, 10 mM imidazole, 2 mM 2-mercaptoethanol (2-ME)], and eluted with a gradient from 0 to 100% of buffer A2 containing 150 mM imidazole. Fractions were analyzed on 4 to 12% Bis-Tris Novex gels (Invitrogen) with MOPS buffer. The protein complex was further purified on a 5-ml HiTrap Q-HP column (GE Healthcare) with buffer C [20 mM Tris (pH 8), 2 mM dithiothreitol (DTT)], and was eluted with buffer D [20mM Tris (pH 8), 2 mM DTT, 1 M NaCl]. The complex was concentrated with AMICON 50K centrifugal filters (Millipore) and loaded onto a 16/60 Superdex 200 gel filtration column (GE Healthcare) at 4°C running with buffer E [20 mM Hepes (pH 7.5), 100 mM NaCl, 2 mM Tris(2-carboxyethyl)phosphine (TCEP)]. The heterodimer was concentrated to about 5 mg/ml, frozen in liquid nitrogen, and stored at -80°C .

Purification of p110 β -p85 α dimers from mammalian cells

HEK 293T cells were cotransfected with plasmids encoding myc-p110 β and p85 α , and the proteins were co-immunoprecipitated with anti-myc antibody. Pellets were washed sequentially three times in PBS containing 1% NP-40, three times in 50 mM Tris(pH 7.4), 500 mM LiCl₂, and twice in 20 mM Tris (pH 7.5), 100 mM NaCl, 1 mM EDTA. Pellets were resuspended in a final volume of 50 μ l of 40 mM HEPES (pH 7.4), 0.1 % bovine serum albumin, 1 mM EGTA, 7 mM MgCl₂, 120 mM NaCl, 1 mM DTT, and 1 mM β -glycerophosphate.

Purification of G β γ expressed in insect cells

Recombinant human G β ₁, N-terminally hexahistidine-tagged bovine wild-type G γ ₂, and the G γ ₂(C68S) mutant were produced in Sf9 cells and purified as described previously [28]. Isoprenylated G β ₁His- γ 2 was isolated from the membrane fraction. The membrane extract was clarified by ultracentrifugation at 100,000g for 1 hour, and diluted five times with a buffer containing 20 mM Hepes-NaOH (pH 7.7), 100 mM NaCl, 0.1 % polyoxyethylene-10-lauryl ether (C12E10), and 10 mM 2-ME. The extract was supplemented with 25 mM imidazole and incubated with Ni²⁺-NTA Superflow beads (Qiagen) for 1 hour. The mixture was loaded onto a column cartridge and extensively washed with buffer containing 20 mM imidazole. Thereafter, bound insect G α subunits were eluted with AlCl₃ in the presence of Mg²⁺. Subsequently, G β ₁His- γ 2 dimers were eluted with a buffer containing 20 mM Tris-HCl (pH 8.0), 25 mM NaCl, 0.1 % C12E10, 200 mM imidazole, and 10 mM 2-ME. G β ₁His- γ 2 eluted from the Ni²⁺-NTA matrix was diluted and loaded onto a 1-ml Resource 15Q HR 5/5 column (GE Healthcare) equilibrated with a buffer containing 20 mM Tris-HCl (pH 8.0), 8 mM CHAPS, and 2 mM DTT. Bound proteins were eluted and fractionated with a continuous gradient elution (0 to 500 mM NaCl). Peak fractions were pooled and concentrated with Amicon 10 concentrators (Millipore). The protein was then loaded onto a gel filtration Superdex 200 HR 10/30 column (GE Healthcare) and eluted with a buffer containing 20 mM Hepes-NaOH (pH 7.7), 100 mM NaCl, 10 mM CHAPS, and 2 mM TCEP. Peak fractions were pooled and concentrated with Amicon 10 concentrators (Millipore). Purified proteins were quantified by Coomassie Brilliant Blue staining after SDS-PAGE analysis with BSA as a standard. Proteins were stored at -80°C . Non-lipidated G β ₁His- γ 2(C68S) was purified from the cytosolic fraction of Sf9 cells. After separation from the membrane fraction, the cytosolic fraction was supplemented with 15 mM imidazole and incubated with Ni²⁺-NTA Superflow beads (Qiagen) for 1 hour. The mixture was loaded onto a column cartridge and extensively washed with a buffer containing 20 mM Hepes-NaOH (pH 7.7), 300 mM NaCl, 15 mM imidazole, and 10 mM 2-ME. G β ₁His-

$\gamma 2$ (C68S) mutants were eluted with a buffer containing 20 mM Tris-HCl (pH 8.0), 25 mM NaCl, 200 mM imidazole, and 10 mM 2-ME. The protein eluted from the Ni²⁺-NTA matrix was diluted and loaded onto a 1-ml Resource 15Q HR 5/5 column (GE Healthcare) equilibrated with a buffer containing 20 mM Tris-HCl (pH 8.0) and 2 mM DTT. Bound proteins were eluted and fractionated with a continuous NaCl gradient elution (0 to 600 mM NaCl). Peak fractions were pooled and concentrated with Amicon 10 concentrators (Millipore). The protein was then loaded onto a gel filtration Superdex 200 HR 10/30 column (GE Healthcare) and eluted with a buffer containing 20 mM Hepes-NaOH (pH 7.7), 100 mM NaCl, and 2 mM TCEP. Peak fractions were pooled and concentrated with Amicon 10 concentrators (Millipore). Purified proteins were quantified by Coomassie Brilliant Blue staining following SDS-PAGE with BSA as a standard. Proteins were stored at -80°C .

Preparation of lipid vesicles

For assays with immunopurified material from mammalian cells, lipid vesicles consisting of 38% phosphatidylethanolamine (PE), 35.5% phosphatidylserine (PS), 16.3% phosphatidylcholine (PC), 3.5% sphingomyelin, and 6.7% phosphatidylinositol-4,5-bisphosphate (PIP₂) (all percentages by weight) [42] were dried under argon, resuspended at 0.66 $\mu\text{g}/\mu\text{l}$ in 40 mM HEPES (pH 7.4), 0.1 % BSA, 1 mM EGTA, 7 mM MgCl₂, 120 mM NaCl, 1 mM DTT, and 1 mM β -glycerophosphate and were sonicated in a Branson cup sonicator. For assays with recombinant protein purified from insect cells, vesicles were prepared by adding the lipid components together in chloroform and evaporating the organic solvent under a stream of dry argon. The lipid film was allowed to dry for 30 min under vacuum, and was then resuspended in a solution of 20 mM Tris (pH 7.5), 100 mM KCl, 1 mM EGTA. The lipids were first bath-sonicated for 10 min, and then subjected to 10 cycles of freeze-thaw between liquid nitrogen and a 37°C water bath. The liposomes were finally extruded ten times through a 100-nm filter (Whatman, Anotop 10) with a gas-tight syringe. Vesicles were frozen at -80°C for storage and were used within 1 month of preparation. Vesicle composition was 5% Brain-PIP₂ (Sigma), 20% Brain-PS (Sigma), 45% brain-PE (Avanti), 15% Dioleoyl-PC (Avanti), 10% cholesterol (Sigma), 5% egg-sphingomyelin (Sigma). Percentages are based on weight.

Assay of lipid kinase activity with immunopurified enzyme

For assays with immunoprecipitated enzymes, myc-tagged wild-type or ⁵³²KK-DD mutant p110 β together with p85 α were coimmunoprecipitated with an anti-myc antibody from appropriately transfected HEK 293T cells. For assays with G $\beta\gamma$, G $\beta\gamma$ was preincubated with lipid vesicles for 30 min and then added to the resuspended enzyme pellets [44]. For assays with phosphopeptide, 1 μM (final concentration) tyrosyl phosphorylated peptide [mouse PDGFR residues 735 to 767, sequence: ESDGG(pY)MDMSKDESID(pY)VPMLDMKGDIKYADIE; referred to as pY] and lipid vesicles were added directly. The assay (immunoprecipitated enzyme and 200 nM G $\beta\gamma$, 320 μM PE, 300 μM PS, 140 μM PC, 30 μM Sphingomyelin, and 300 μM PI in a final volume of 81 μl) was initiated by the addition of 5 μl of ATP (116 μM final concentration) containing 1 μCi [³²P]ATP. After 10 min at 22°C, the assay was stopped by the addition of EDTA (50 μM final concentration), and 5- μl aliquots were spotted on nitrocellulose membranes. The membranes were washed 5 times in 1 M NaCl, containing 1% phosphoric acid, dried, and counted with a Molecular Dynamics Phosphorimager. Alternatively, assays were analyzed by thin layer chromatography by stopping the reaction with 20 μl of 7N HCl, mixing with 160 μl of a 1:1 solution of methanol:chloroform, and centrifugation to separate the phases, after which, 20 μl of the organic phase was spotted onto a silica gel plate (EMD Merck). Plates were developed in a solvent system consisting of 60 ml of chloroform, 47 ml of methanol, 11.2 ml water, and 2 ml of ammonium hydroxide, dried, and counted with a Molecular Dynamics Phosphorimager. For assays using the inhibitory peptides, a 1 μM final

concentration of peptides (WT p110 β : KAAEIASSDSANVSSRGGKKFLPV; scrambled p110 β : NGAEKVGSADSKSIAFVSLKARSP) in 20 mM Tris-HCl (pH 7.4), 10 mM NaCl was incubated with 200 nM of G $\beta\gamma$ for 30 min on ice, and then with lipids, as described earlier, for 10 min on ice, and finally for 10 min with immunopurified PI3K, after which the kinase assay described earlier was performed. For assays of immunopurified PI3K γ in the presence of peptide, peptides (1 μ M WT p110 β ; 1 μ M scrambled p110 β ; 10 μ M SIGK: SIGKAFKILGYPDYD; or 1 μ M QEHA: QEHAQEPERQYMHIGTMVEFAYALVGK) in 20 mM Tris-HCl (pH 7.4), 10 mM NaCl was incubated with 200 nM of G $\beta\gamma$ for 30 min on ice, and was then incubated with lipids as described earlier for 10 min on ice, before finally being incubated for 10 min with immunopurified PI3K γ from baculovirus-infected insect cells, after which the kinase assay described above was performed.

Assay of lipid kinase activity with enzyme purified from insect cells

For assays with recombinant PI3K from baculovirus-infected insect cells, lipid vesicles were used at a final concentration of 1 mg/ml and were prepared as described earlier. Stock solutions of three-fold concentrated WT or mutant PI3K β constructs were prepared at 75 nM (for assays of basal, pY-stimulated, and G $\beta\gamma$ -stimulated activity) and at 0.75 nM (for assay of synergistic activation by pY and G $\beta\gamma$) in 20 mM Hepes (pH 7.5), 100 mM NaCl, 2 mM DTT, 9 mM MgCl₂, 3 mM EDTA. Substrate stock solutions containing lipids (3 mg/ml) supplemented with either 900 nM RTK-pY [from a 100 μ M stock in 10 mM Hepes (pH 7.5), 0.2% DMSO], 1.5 μ M G $\beta_1\gamma_2$ [from a 50 μ M stock in 20 mM Hepes (pH 7.5), 100 mM NaCl, 2 mM TCEP, 10 mM CHAPS], or both agonists were prepared in 20 mM Hepes (pH 7.5), 100 mM NaCl, 2 mM DTT. The concentrations of CHAPS and DMSO were adjusted to be equal under all conditions. A 300 μ M ATP solution containing 0.1 mCi/ml of [γ ³²P]-ATP was prepared. The reaction was started by mixing 3 μ l of protein stock with 3 μ l of substrate stock and 3 μ l of ATP solution. The reaction was stopped after 60 min by transferring 3 μ l of reaction mixture to 3 μ l of a 20 mM EDTA quench buffer. Lipid kinase activity was determined with a modified membrane-capture radioactive assay measuring the production of ³²P-labeled PIP₃ [43]. Three microliters of this mixture was then spotted on a nitrocellulose membrane. The membrane was dried and washed six times with 1 M NaCl, containing 1% phosphoric acid. The membrane was then air-dried before exposure to a phosphor screen (Molecular Dynamics) for 15 min. The intensity of the spots on the membrane was imaged with a Typhoon Phosphorimager (GE Healthcare) and quantified with ImageQuant software (GE Healthcare).

HDX-MS measurements

HDX-MS analyses of PI3K β and G $\beta\gamma$ were performed by following a similar protocol as that previously described [16]. In the experiment identifying interaction sites between PI3K β and soluble G $\beta\gamma$ -C68S, the rate of exchange of the p110 β -G β_1 -p85 α -icSH2-G γ_2 -C68S fusion heterotrimer was compared to those of a p110 β -p85 α -icSH2 free heterodimer and a free G $\beta_1\gamma_2$ -C68S heterodimer. Protein stock solutions at 7 μ M were prepared in 20 mM Hepes (pH 7.5), 100 mM NaCl and 2 mM DTT. Exchange reactions were started by mixing 10 μ l of protein stock with 40 μ l of a 98% D₂O solution containing 10 mM HEPES (pH 7.5), 50 mM NaCl, reaching a final concentration of 78% D₂O. Deuterium exchange reactions were run for 3, 30, 300, and 3000 s of on-exchange at 23°C before the reactions were quenched. An additional experiment for 3 s of on-exchange was performed at 0°C to examine exchange rates of very rapidly exchanging hydrogens. On-exchange was stopped with 20 μ l of quench buffer containing 1.2% formic acid and 2 M Guanidine-HCl, which lowered the pH to 2.6. Samples were then immediately frozen in liquid nitrogen and stored at -80°C for no longer than 7 days. For HDX-MS studies in the presence of lipids, on-exchange experiments were performed in the presence of 10 μ M PDGFR pY. Lipid vesicles at 5 mg/ml were diluted 8-fold with the 98% D₂O solution described earlier. Protein stock

solutions containing 10 μM of pY [40 μM stock in 10 mM HEPES (pH 7.2), 0.08 % DMSO] were prepared and incubated for 10 min before the addition of deuterated buffer. To shift the equilibrium toward the PI3K β -lipidated G $\beta\gamma$ complex and minimize the concentration of free p110 β -p85 heterodimer, the G $\beta\gamma$ concentration used (10 μM) was in excess of the PI3K β concentration (3 μM). PI3K β -pY (state 1), in the presence of lipids (state 2), and in the presence of lipids and G $\beta\gamma$ (state 3) were used in this set of experiments to differentiate between changes in the exchange of PI3K β arising from membrane interaction and those from G $\beta\gamma$ interaction. Exchange reactions were started by the addition of 10 μl of protein stock to 40 μl of lipid-containing D₂O solution, reaching a final concentration of 69% D₂O. Deuterium exchange reactions ran for the same time points described for experiments with the fusion construct, but no measurements were performed at 0°C because of problems with lipid precipitation. Samples were stored at -80°C for a maximum of 1 week before deuterium incorporation was measured. Every time point and state was a unique experiment, and every HDX-MS experiment was repeated twice.

Measurement of deuterium incorporation

Samples were rapidly thawed on ice and injected onto a ultra-performance liquid chromatography (UPLC) system immersed in ice. The protein was run over an immobilized pepsin column (Applied Biosystems, Poroszyme, 2-3131-00) at 130 $\mu\text{l}/\text{min}$, and collected over a particle van-guard pre column (Waters) for 3 min. The trap was then eluted in line with an Acquity 1.7 μm -particle, 100 mm \times 1 mm C18 UPLC column (Waters) with a 5 to 36% gradient of buffer A (0.1% formic acid) and buffer B (100% acetonitrile) over 20 min, and injected onto a LTQ Orbitrap XL (Thermo Scientific) to acquire mass spectra of peptides ranging from 350 to 1500 m/z.

Protein digestion and peptide identification

Mass analysis of the peptide centroids was performed as described previously, using the software HD-Examiner (Sierra Analytics) [16]. Initial peptide identification was done by running tandem MS/MS experiments using a 5 to 35% B gradient over 60 min with an LTQ Orbitrap XL (Thermo Scientific). Peptides were identified by Mascot search in Thermo Proteome Discoverer software v. 1.2 (Thermo Scientific) based on fragmentation and peptide mass. The MS tolerance was set at 3 ppm, with a MS/MS tolerance of 0.5 Daltons. All peptides with a Mascot score >15 were analyzed by the HD-Examiner software. Any ambiguous peptides were excluded from the analysis. The full list of peptides was then manually validated by searching a non-deuterated protein sample MS scan to test for correct m/z state, and to check for the presence of overlapping peptides. The HD-Examiner software was used to automate the initial analysis of deuterium incorporation, but every peptide listed in the manuscript was manually verified at every state and time to check for correct charge state, m/z range, presence of overlapping peptides, and proper retention time.

Mass analysis of peptide centroids

Selected peptides were manually examined for deuterium incorporation and accurate identification. Results are presented as relative extent of deuteration with no correction for back exchange, because no fully deuterated protein sample could be obtained. However, a correction was applied to compensate for differences in the amount of deuterium in the exchange buffer (78 or 69% in experiments with lipids). The real extent of deuteration was ~25 to 35% higher than what is shown, based on tests performed with fully deuterated standard peptides. The average error was 0.2 Daltons for corrected data of two replicates. The deuterium incorporation was also plotted versus the on-exchange time. The 3 s at 0°C time point was labeled as 0.3 sec. Because we performed the experiments with lipids at lower protein concentration to increase the lipid to protein ratio, some peptides analyzed for the fusion construct could no longer be analyzed.

Akt activation

HEK 293T or HEK 293E cells were grown in Dulbecco's modified Eagle's medium (DMEM) containing 10% fetal bovine serum (FBS) and transfected with plasmids encoding human p85 α , wild-type (WT) or mutant human myc-p110 β , myc-Akt with or without plasmids encoding FLAG-tagged G β ₁ (FLAG-G β ₁) and hemagglutinin (HA)-tagged G γ ₂ (HA-G γ ₂), as indicated. Cells were incubated overnight in serum-free medium. N-myristoylated peptides (WT: KAAEIASSDSANVSSRGGKKFLPV; scrambled: NGAEKVGSADSKSIAFVSLKARSP; 50 mM stock in DMSO; final concentration: 30 μ M), wortmannin (100 nM), PIK-75 (10 nM), and TGX-221 (50 nM) were added to the medium for 30 min before lysis of cells. After incubation, cells were lysed and subjected to immunoprecipitation with anti-myc antibodies. Lysates and immunoprecipitates were analyzed by Western blotting for Akt and pT308-Akt with specific antibodies (Cell Signaling Technologies), and were analyzed by ECL (GE Healthcare) followed by densitometry, or with the LICOR Odyssey imaging system. Results are shown as the ratio of the abundance of pAkt to that of total Akt.

Transformation assays

NIH 3T3 cells grown in DMEM containing 10% normal calf serum (NCS) were transfected with plasmids encoding p110 β and p85 α constructs. Two days after transfection, cells (2,500 cells/well) were plated in 1 ml of 0.3% top agar over 1 ml of 0.6% bottom agar in a six-well dish. Cell colonies were counted 3 weeks later. In assays with the myristoylated peptides, peptides were diluted to a concentration of 30 μ M in both the top and bottom gels as well as in the media.

Focus formation assays

NIH 3T3 cells were plated (at 2×10^5 cells/well) in 6-well dishes and were transfected with plasmids encoding myc-p110 β and p85 α constructs. Cells were grown for two weeks, with media changed every two days. The cells were fixed and stained with crystal violet, and the numbers of foci per well were counted. In assays with the myristoylated peptides, peptides were diluted to a concentration of 30 μ M in the media for the duration of the assay.

Rab5 pulldown assays

HEK 293T cells were transfected with Fugene HD with plasmids encoding WT or mutant myc-p110 β and p85 α . The cells were washed with cold PBS and lysed in 120 mM NaCl, 20 mM Tris (pH 7.5), 1 mM MgCl₂, 1 mM CaCl₂, 10% glycerol, 1% NP40, containing EDTA-free Protease inhibitor cocktail (Roche) and Phosphatase inhibitor cocktails 1 (EMD) and 2 (Sigma). Lysates were incubated with GTP γ S-Rab5 or glutathione-S-transferase (GST) beads as described previously [45] and washed, and bound proteins were eluted and analyzed by Western blotting.

Boyden chamber assays

NIH3T3 cells, NIH3T3 cells stably expressing WT or mutant p110 β , or PC-3 cells were plated at 5×10^4 cells on tissue culture inserts containing 8.0 μ m pores. The inserts were incubated with serum-free media in the presence of DMSO or myristoylated peptides (30 μ M) in the upper chamber and media containing DMSO or peptides with 10% FBS in the lower chamber. After 24 hours, the cells were fixed in 4% paraformaldehyde. The insert membranes were removed, stained and mounted on coverslips with Dapi Fluoromount (Southern Biotech). Images were collected at 10x magnification with a Nikon Diaphot inverted fluorescence microscope and a SPOT Idea digital camera, and were analyzed using ImageJ software.

MTT cell proliferation assays

The MTT assay (Invitrogen) was performed as described by the manufacturer. Briefly, 1×10^3 cells were plated in 96-well plates in the appropriate medium with or without DMSO or 30 μ M myristoylated peptides. At various times, the cells were incubated with a 12 mM MTT solution in PBS for 4 hours at 37°C. An equal volume of 0.1 g/ml SDS solution in 0.01 M HCl was added, and absorbance was read at 570 nm with a Spectramax M5 plate reader (Molecular Devices). The number of cells was calculated from the ratio of OD:cell number from a known number of cells on day 1.

Collagen invasion Assay

BAC-1.2F5 macrophages and PC-3 tumor cells were vitally-labeled with CellTracker Red CMPTX and CellTracker Green CMFDA, respectively, and co-cultured at a 2.5:1 ratio in a MatTek plate. After cell attachment, the cells were overlaid with a collagen I gel. Invasion into the 3D gel was quantified after 24 hours by laser scanning confocal microscopy detection of the fluorescent signal from the red and green CellTracker dyes as described previously [31].

Adenylyl cyclase assay

Sf9 cells were infected with baculovirus coding for recombinant adenylyl cyclase 2. Sf9 cell membranes containing adenylyl cyclase 2 were prepared as previously described [46]. Adenylyl cyclase activity was measured with the procedure described by Smigel [47]. All assays were performed for 10 min at 30°C in a final volume of 100 μ l containing 5 μ g of cyclase-containing Sf9 membrane protein, 20 nM each of recombinant $G_{\alpha s}$ and $G_{\beta\gamma}$, and 30 μ M of myristoylated p110 β peptide or a previously described inhibitory QEHA peptide (QEHAQEPERQYMHIGTMVEFAYALVGK) [48]. The data are mean \pm the standard deviation (SD) from duplicate determinations, and are representative of two separate experiments.

LC3 punctae assays

HEK 293A cells stably expressing green fluorescent protein (GFP)-tagged LC3 were plated on poly-L-lysine-coated coverslips, treated with DMSO or myristoylated peptides (30 μ M) for 30 min, and then incubated in PBS, 100 nM rapamycin and peptide for 2 hours at 37°C. Coverslips were fixed in 4% PFA for 10 min at room temperature, and then imaged with 60 \times 1.4 N.A. optics with a Nikon Eclipse E400 microscope. Images were collected with a Roper cooled CCD camera and analyzed using ImageJ software.

In vitro activation of PLC β

L- α -phosphatidylethanolamine (Avanti Polar Lipids, bovine liver), L- α -phosphatidylinositol-4,5-bisphosphate (Avanti, porcine brain) and [3 H] phosphatidylinositol-4,5-bisphosphate (NEN Radiochemicals) were combined in chloroform, dried under a stream of N_2 , and resuspended in 20 mM Hepes (pH 7.2) by sonication. Recombinant PLC β 3 (1 nM) was incubated with the indicated concentrations of p110 β peptide, scrambled peptide, or SIGK peptide, with or without 200 nM $G_{\alpha q}$ and in the presence or absence of 60 nM $G_{\beta\gamma}$, for 10 min at 30°C in a final volume of 60 μ l containing 20 mM Hepes (pH 7.2), 8.3 mM NaCl, BSA (0.167 mg/ml), 2 mM DTT, 70 mM KCl, 3 mM EGTA, 10 mM NaF, 20 μ M $AlCl_3$, 5 mM $MgCl_2$, 33 μ M PIP_2 , 333 μ M PE, 10,000 to 15000 dpm [3 H] PIP_2 and $CaCl_2$ added to give a free concentration of 200 nM Ca^{2+} . The assay was terminated by the addition of 200 μ l of 10% TCA and 100 μ l of BSA (10 mg/ml), followed by centrifugation for 10 min at 4500 g. The supernatant was quantified by liquid scintillation spectrometry.

Quantification of [³H]inositol phosphate accumulation in cells

COS-7 cells were transiently transfected with or without plasmids encoding Gβγ subunits with Fugene 6. The culture medium was changed approximately 48 hours after plating to inositol-free DMEM (MP Biomedical) containing 1 μCi/well [2-³H(N)]myo-inositol (American Radiolabeled Chemicals). Metabolic labeling proceeded for 18 hours, at which point 100 μl of myristoylated or TAT-labeled peptide (to a final concentration of 30 μM) was added. After 30 min, 50 mM LiCl in 20 mM HEPES (pH 7.2) was added for 1 hour at 37°C. Incubations were terminated by aspiration of media and the addition of ice-cold 50 mM formic acid, followed by neutralization with 150 mM NH₄OH after cell lysis. [³H]Inositol phosphates were isolated and quantified by Dowex chromatography. Parallel dishes were lysed and assayed for Akt activation as described earlier.

Statistical analysis

Error bars show the SEM for experiments performed three or more times, and the SD for experiments performed twice. Statistical analyses were performed by ANOVA.

Supplementary Material

Refer to Web version on PubMed Central for supplementary material.

Acknowledgments

We thank C. S. Rubin, S. C. Almo, J. B. Bonnano, and P. Seneviratne for valuable discussions; M. Levy for the PC3 cell line; S. Tooze for the GFP-LC3 stable cell line; and S. B. Horwitz for the panel of endometrial cancer cell lines. We also thank F. Begum and S.-Y. Peak-Chew for help with the HDX-MS setup, J. Morrow for assistance with HD-examiner software, and R. Riehle for technical assistance with the purification of proteins.

Funding: O.V. was supported by a Swiss National Science Foundation fellowship (grant No PA00P3_134202) and a European Commission fellowship (FP7-PEOPLE-2010-IEF, N°275880). J.E B. was supported by an EMBO long-term fellowship (ALTF268-2009) and the British Heart Foundation (PG11/109/29247). H.A D. and B.D.K. were supported by grants from the Janey Fund. R.S S. was supported by NIH 5T32 GM007491 and by a National Research Service Award, 1 F31 AG040932-01. T.K.H. was supported by NIH grant GM57391. This work was funded by NIH grants GM55692 (to J.M.B.) and PO1 CA 100324 (to J.M.B. and A.R.B.), by the Medical Research Council (to R.L.W., file reference U105184308) and by Deutsche Forschungsgemeinschaft (to B.N).

References and Notes

- Engelman JA. Targeting PI3K signalling in cancer: opportunities, challenges and limitations. *Nat Rev Cancer*. 2009; 9:550–562. [PubMed: 19629070]
- Yu J, Zhang Y, McIlroy J, Rordorf-Nikolic T, Orr GA, Backer JM. Regulation of the p85/p110 phosphatidylinositol 3'-kinase: Stabilization and inhibition of the p110-alpha catalytic subunit by the p85 regulatory subunit. *Mol Cell Biol*. 1998; 18:1379–1387. [PubMed: 9488453]
- Geering B, Cutillas PR, Nock G, Gharbi SI, Vanhaesebroeck B. Class IA phosphoinositide 3-kinases are obligate p85-p110 heterodimers. *Proc Natl Acad Sci U S A*. 2007; 104:7809–7814. [PubMed: 17470792]
- Kulkarni S, Sitaru C, Jakus Z, Anderson KE, Damoulakis G, Davidson K, Hirose M, Juss J, Oxley D, Chessa TA, Ramadani F, Guillou H, Segonds-Pichon A, Fritsch A, Jarvis GE, Okkenhaug K, Ludwig R, Zillikens D, Mocsai A, Vanhaesebroeck B, Stephens LR, Hawkins PT. PI3Kbeta plays a critical role in neutrophil activation by immune complexes. *Sci Signal*. 2011; 4:ra23. [PubMed: 21487106]
- Kurosu H, Maehama T, Okada T, Yamamoto T, Hoshino S, Fukui Y, Ui M, Hazeki O, Katada T. Heterodimeric phosphoinositide 3-kinase consisting of p85 and p110β is synergistically activated by the βgamma subunits of G proteins and phosphotyrosyl peptide. *J Biol Chem*. 1997; 272:24252–24256. [PubMed: 9305878]

6. Murga C, Fukuhara S, Gutkind JS. A novel role for phosphatidylinositol 3-kinase beta in signaling from G protein-coupled receptors to Akt. *J Biol Chem.* 2000; 275:12069–12073. [PubMed: 10766839]
7. Maier U, Babich A, Nürnberg B. Roles of non-catalytic subunits in G β gamma-induced activation of class I phosphoinositide 3-kinase isoforms β and γ . *J Biol Chem.* 1999; 274:29311–29317. [PubMed: 10506190]
8. Wee S, Wiederschain D, Maira SM, Loo A, Miller C, deBeaumont R, Stegmeier F, Yao YM, Lengauer C. PTEN-deficient cancers depend on PIK3CB. *Proc Natl Acad Sci U S A.* 2008; 105:13057–13062. [PubMed: 18755892]
9. Berenjeno IM, Guillermet-Guibert J, Pearce W, Gray A, Fleming S, Vanhaesebroeck B. Both p110alpha and p110beta isoforms of PI3K can modulate the impact of loss-of-function of the PTEN tumour suppressor. *Biochem J.* 2012; 442:151–159. [PubMed: 22150431]
10. Jia S, Liu Z, Zhang S, Liu P, Zhang L, Lee SH, Zhang J, Signoretti S, Loda M, Roberts TM, Zhao JJ. Essential roles of PI(3)K-p110beta in cell growth, metabolism and tumorigenesis. *Nature.* 2008; 454:776–779. [PubMed: 18594509]
11. Ni J, Liu Q, Xie S, Carlson C, Von T, Vogel K, Riddle S, Benes C, Eck M, Roberts T, Gray N, Zhao J. Functional Characterization of an Isoform-Selective Inhibitor of PI3K-p110beta as a Potential Anticancer Agent. *Cancer discovery.* 2012; 2:425–433. [PubMed: 22588880]
12. Songyang Z, Shoelson SE, Chaudhuri M, Gish G, Pawson T, Haser WG, King F, Roberts T, Ratnofsky S, Lechleider RJ, Neel BG, Birge RB, Fajardo JE, Chou MM, Hanafusa H, Schaffhausen B, Cantley LC. SH2 domains recognize specific phosphopeptide sequences. *Cell.* 1993; 72:767–778. [PubMed: 7680959]
13. O'Brien R, Rugman P, Renzoni D, Layton M, Handa R, Hilyard K, Waterfield MD, Driscoll PC, Ladbury JE. Alternative modes of binding of proteins with tandem SH2 domains. *Protein Sci.* 2000; 9:570–579. [PubMed: 10752619]
14. Dbouk HA, Pang H, Fiser A, Backer JM. A biochemical mechanism for the oncogenic potential of the p110beta catalytic subunit of phosphoinositide 3-kinase. *Proc Natl Acad Sci U S A.* 2010; 107:19897–19902. [PubMed: 21030680]
15. Zhang X, Vadas O, Perisic O, Anderson KE, Clark J, Hawkins PT, Stephens LR, Williams RL. Structure of Lipid Kinase p110beta/p85beta Elucidates an Unusual SH2-Domain-Mediated Inhibitory Mechanism. *Mol Cell.* 2011; 41:567–578. [PubMed: 21362552]
16. Burke JE, Vadas O, Berndt A, Finegan T, Perisic O, Williams RL. Dynamics of the phosphoinositide 3-kinase p110delta interaction with p85alpha and membranes reveals aspects of regulation distinct from p110alpha. *Structure.* 2011; 19:1127–1137. [PubMed: 21827948]
17. Chung KY, Rasmussen SG, Liu T, Li S, DeVree BT, Chae PS, Calinski D, Kobilka BK, Woods VL Jr, Sunahara RK. Conformational changes in the G protein Gs induced by the beta2 adrenergic receptor. *Nature.* 2011; 477:611–615. [PubMed: 21956331]
18. Engen JR. Analysis of protein conformation and dynamics by hydrogen/deuterium exchange MS. *Anal Chem.* 2009; 81:7870–7875. [PubMed: 19788312]
19. Burke JE, Perisic O, Masson GR, Vadas O, Williams RL. Oncogenic mutations mimic and enhance dynamic events in the natural activation of phosphoinositide 3-kinase p110alpha (PIK3CA). *Proc Natl Acad Sci U S A.* 2012; 109:15259–15264. [PubMed: 22949682]
20. Zhang X, Vadas O, Perisic O, Anderson KE, Clark J, Hawkins PT, Stephens LR, Williams RL. Structure of lipid kinase p110beta/p85beta elucidates an unusual SH2-domain-mediated inhibitory mechanism. *Mol Cell.* 2011; 41:567–578. [PubMed: 21362552]
21. Mandelker D, Gabelli SB, Schmidt-Kittler O, Zhu J, Cheong I, Huang CH, Kinzler KW, Vogelstein B, Amzel LM. A frequent kinase domain mutation that changes the interaction between PI3Kalpha and the membrane. *Proc Natl Acad Sci U S A.* 2009; 106:16996–17001. [PubMed: 19805105]
22. Sun M, Hart JR, Hillmann P, Gymnopoulos M, Vogt PK. Addition of N-terminal peptide sequences activates the oncogenic and signaling potentials of the catalytic subunit p110alpha of phosphoinositide-3-kinase. *Cell Cycle.* 2011; 10:3731–3739. [PubMed: 22045127]

23. Maier U, Babich A, Macrez N, Leopoldt D, Gierschik P, Illenberger D, Nurnberg B. Gbeta 5gamma 2 is a highly selective activator of phospholipid-dependent enzymes. *J Biol Chem.* 2000; 275:13746–13754. [PubMed: 10788495]
24. Buck E, Li J, Chen Y, Weng G, Scarlata S, Iyengar R. Resolution of a signal transfer region from a general binding domain in gbeta for stimulation of phospholipase C-beta2. *Science.* 1999; 283:1332–1335. [PubMed: 10037604]
25. Panchenko MP, Saxena K, Li Y, Charnecki S, Sternweis PM, Smith TF, Gilman AG, Kozasa T, Neer EJ. Sites important for PLCbeta2 activation by the G protein betagamma subunit map to the sides of the beta propeller structure. *J Biol Chem.* 1998; 273:28298–28304. [PubMed: 9774453]
26. Scott JK, Huang SF, Gangadhar BP, Samoriski GM, Clapp P, Gross RA, Taussig R, Smrcka AV. Evidence that a protein-protein interaction ‘hot spot’ on heterotrimeric G protein betagamma subunits is used for recognition of a subclass of effectors. *EMBO J.* 2001; 20:767–776. [PubMed: 11179221]
27. Li Y, Sternweis PM, Charnecki S, Smith TF, Gilman AG, Neer EJ, Kozasa T. Sites for Galpha binding on the G protein beta subunit overlap with sites for regulation of phospholipase Cbeta and adenylyl cyclase. *J Biol Chem.* 1998; 273:16265–16272. [PubMed: 9632686]
28. Shymanets A, Ahmadian MR, Kossmeier KT, Wetzker R, Harteneck C, Nurnberg B. The p101 subunit of PI3Kgamma restores activation by Gbeta mutants deficient in stimulating p110gamma. *Biochem J.* 2012; 441:851–858. [PubMed: 22054284]
29. Dou Z, Chattopadhyay M, Pan JA, Guerriero JL, Jiang YP, Ballou LM, Yue Z, Lin RZ, Zong WX. The class IA phosphatidylinositol 3-kinase p110-beta subunit is a positive regulator of autophagy. *J Cell Biol.* 2010; 191:827–843. [PubMed: 21059846]
30. Bookout AL, Finney AE, Guo R, Peppel K, Koch WJ, Daaka Y. Targeting Gbetagamma signaling to inhibit prostate tumor formation and growth. *J Biol Chem.* 2003; 278:37569–37573. [PubMed: 12869546]
31. Goswami S, Sahai E, Wyckoff JB, Cammer M, Cox D, Pixley FJ, Stanley ER, Segall JE, Condeelis JS. Macrophages promote the invasion of breast carcinoma cells via a colony-stimulating factor-1/epidermal growth factor paracrine loop. *Cancer Res.* 2005; 65:5278–5283. [PubMed: 15958574]
32. Lappano R, Maggiolini M. G protein-coupled receptors: novel targets for drug discovery in cancer. *Nat Rev Drug Discov.* 2011; 10:47–60. [PubMed: 21193867]
33. Dorsam RT, Gutkind JS. G-protein-coupled receptors and cancer. *Nat Rev Cancer.* 2007; 7:79–94. [PubMed: 17251915]
34. Daaka Y. G proteins in cancer: the prostate cancer paradigm. *Sci STKE.* 2004; 2004:re2. [PubMed: 14734786]
35. Macrez N, Mironneau C, Carricaburu V, Quignard JF, Babich A, Czupalla C, Nurnberg B, Mironneau J. Phosphoinositide 3-kinase isoforms selectively couple receptors to vascular L-type Ca(2+) channels. *Circ Res.* 2001; 89:692–699. [PubMed: 11597992]
36. Jackson SP, Schoenwaelder SM, Goncalves I, Nesbitt WS, Yap CL, Wright CE, Kenche V, Anderson KE, Dopheide SM, Yuan Y, Sturgeon SA, Prabakaran H, Thompson PE, Smith GD, Shepherd PR, Daniele N, Kulkarni S, Abbott B, Saylik D, Jones C, Lu L, Giuliano S, Hughan SC, Angus JA, Robertson AD, Salem HH. PI 3-kinase p110beta: a new target for antithrombotic therapy. *Nat Med.* 2005; 11:507–514. [PubMed: 15834429]
37. Ciralo E, Morello F, Hobbs RM, Wolf F, Marone R, Iezzi M, Lu X, Mengozzi G, Altruda F, Sorba G, Guan K, Pandolfi PP, Wymann MP, Hirsch E. Essential role of the p110beta subunit of phosphoinositide 3-OH kinase in male fertility. *Mol Biol Cell.* 2010; 21:704–711. [PubMed: 20053680]
38. Leverrier Y, Okkenhaug K, Sawyer C, Bilancio A, Vanhaesebroeck B, Ridley AJ. Class I phosphoinositide 3-kinase p110beta is required for apoptotic cell and Fcgamma receptor-mediated phagocytosis by macrophages. *J Biol Chem.* 2003; 278:38437–38442. [PubMed: 12869549]
39. Jackson SP, Schoenwaelder SM. PI 3-Kinase p110beta regulation of platelet integrin alpha(IIb)beta3. *Curr Top Microbiol Immunol.* 2010; 346:203–224. [PubMed: 20517720]
40. Ciralo E, Iezzi M, Marone R, Marengo S, Curcio C, Costa C, Azzolino O, Gonella C, Rubinetto C, Wu H, Dastu W, Martin EL, Silengo L, Altruda F, Turco E, Lanzetti L, Musiani P, Ruckle T, Rommel C, Backer JM, Forni G, Wymann MP, Hirsch E. Phosphoinositide 3-kinase p110beta

- activity: key role in metabolism and mammary gland cancer but not development. *Sci Signal.* 2008; 1:ra3. [PubMed: 18780892]
41. Kumar A, Fernandez-Capetillo O, Carrera AC. Nuclear phosphoinositide 3-kinase beta controls double-strand break DNA repair. *Proc Natl Acad Sci U S A.* 2010; 107:7491–7496. [PubMed: 20368419]
 42. Leopoldt D, Hanck T, Exner T, Maier U, Wetzker R, Nurnberg B. Gbetagamma stimulates phosphoinositide 3-kinase-gamma by direct interaction with two domains of the catalytic p110 subunit. *J Biol Chem.* 1998; 273:7024–7029. [PubMed: 9507010]
 43. Knight ZA, Feldman ME, Balla A, Balla T, Shokat KM. A membrane capture assay for lipid kinase activity. *Nat Protoc.* 2007; 2:2459–2466. [PubMed: 17947987]
 44. Leopoldt D, Hanck T, Exner T, Maier U, Wetzker R, Nurnberg B. Gbetagamma stimulates phosphoinositide 3-kinase-gamma by direct interaction with two domains of the catalytic p110 subunit. *J Biol Chem.* 1998; 273:7024–7029. [PubMed: 9507010]
 45. Christoforidis S, Zerial M. Purification and identification of novel Rab effectors using affinity chromatography. *Methods.* 2000; 20:403–410. [PubMed: 10720461]
 46. Taussig R, Tang WJ, Gilman AG. Expression and purification of recombinant adenylyl cyclases in Sf9 cells. *Methods Enzymol.* 1994; 238:95–108. [PubMed: 7799806]
 47. Smigel MD. Purification of the catalyst of adenylyl cyclase. *J Biol Chem.* 1986; 261:1976–1982. [PubMed: 3080431]
 48. Chen J, DeVivo M, Dingus J, Harry A, Li J, Sui J, Carty DJ, Blank JL, Exton JH, Stoffel RH, et al. A region of adenylyl cyclase 2 critical for regulation by G protein beta gamma subunits. *Science.* 1995; 268:1166–1169. [PubMed: 7761832]

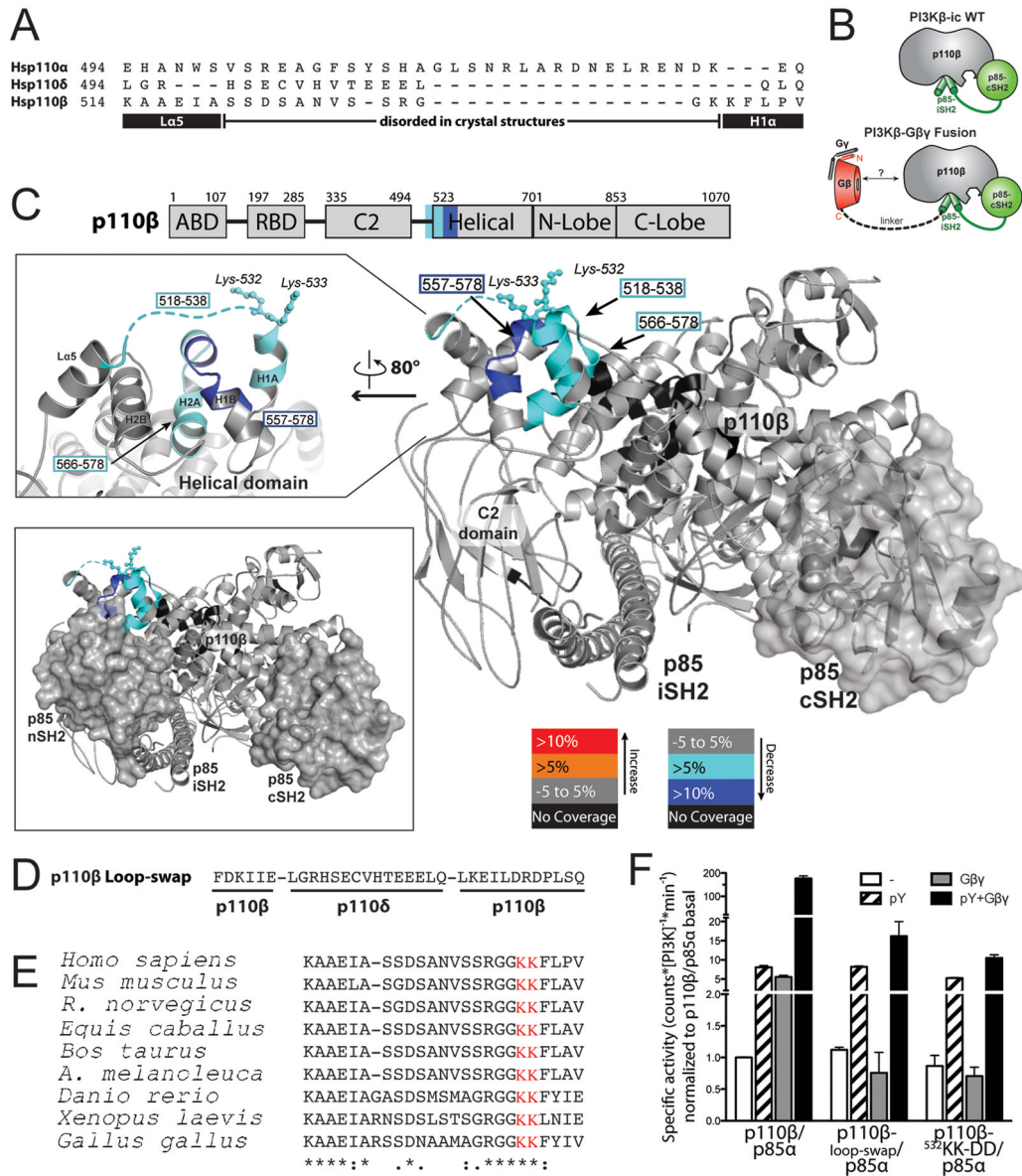


Fig. 1. Mapping of the Gβγ-binding site on p110β by sequence analysis and HDX-MS. (A) Sequence alignment of the C2 domain–helical domain linker region of p110α, β, and δ. The black rectangles denote helices in the p110β structure, and the black line represents the disordered region. (B) Cartoon illustration of the p110β–p85α-icSH2 wild-type (WT) heterodimer and the p110β–Gβ–p85α-icSH2–Gγ-C68S fusion heterotrimer (fusion) used for the HDX-MS experiments. (C) Domains of p110β are outlined and colored according to the legend for changes associated with the presence of Gβγ. Regions in p110β and p85α-icSH2 that showed >0.5 Dalton and >5% changes in deuteration extent between the WT and fusion complexes were mapped on the p110β–p85β-icSH2 model (PDB: 2y3a, right panel). The loop region between the C2 domain and the helical domain is represented as a dotted line because it is not ordered in the structure. Residues corresponding to human p110β K532 and K533 are represented with balls and sticks. Top left, a close-up view of the p110β region in which changes in deuteration extent as a result of the presence of Gβγ were detected is

shown. Bottom left, a model for the p110 β -p85 α -nicSH2 generated by combining the structures of p110 β -p85 β -icSH2 (PDB: 2Y3A) and p85 α -nSH2 (PDB: 3HHM). The nSH2 and cSH2 domains of p85 are shown as surface representations. The p85 α -nSH2 position is based on the structure of p110 α , although there is no unambiguous evidence that nSH2 adopts exactly the same position when in complex with p110 β . **(D)** Sequence of the loop-swap mutant of p110 β . **(E)** Alignment of p110 β zoologs in the region of the C2-helical linker. **(F)** Activities of WT PI3K β and the loop-swap and ⁵³²KK-DD mutants purified from insect cells, in the presence of pY peptide (pY) and lipidated G β γ . Activities were expressed relative to the basal activity of PI3K β , which was normalized to one. Graph shows the activity \pm SD of three independent experiments.

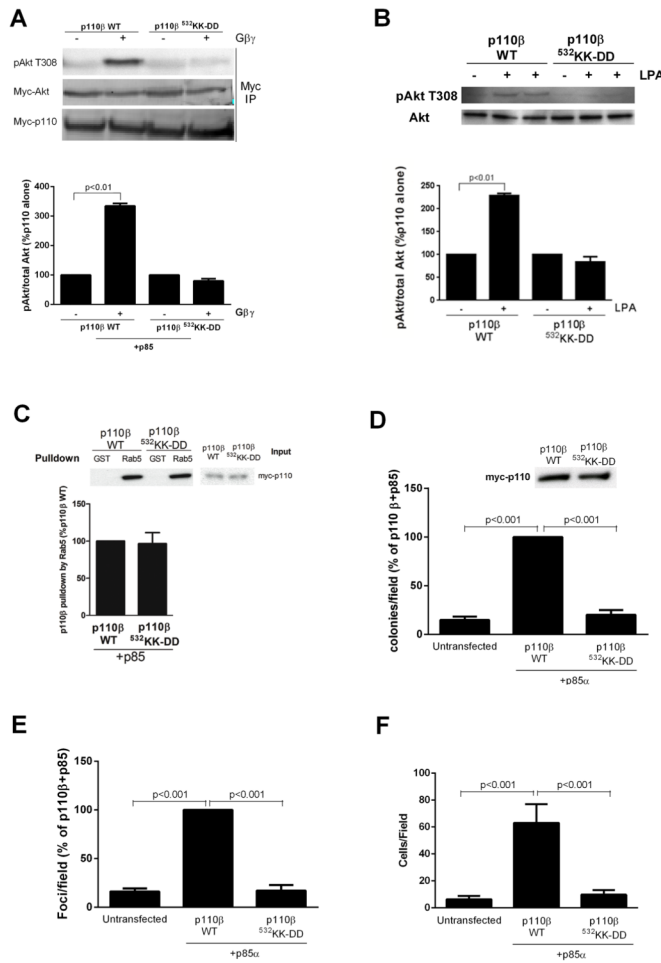
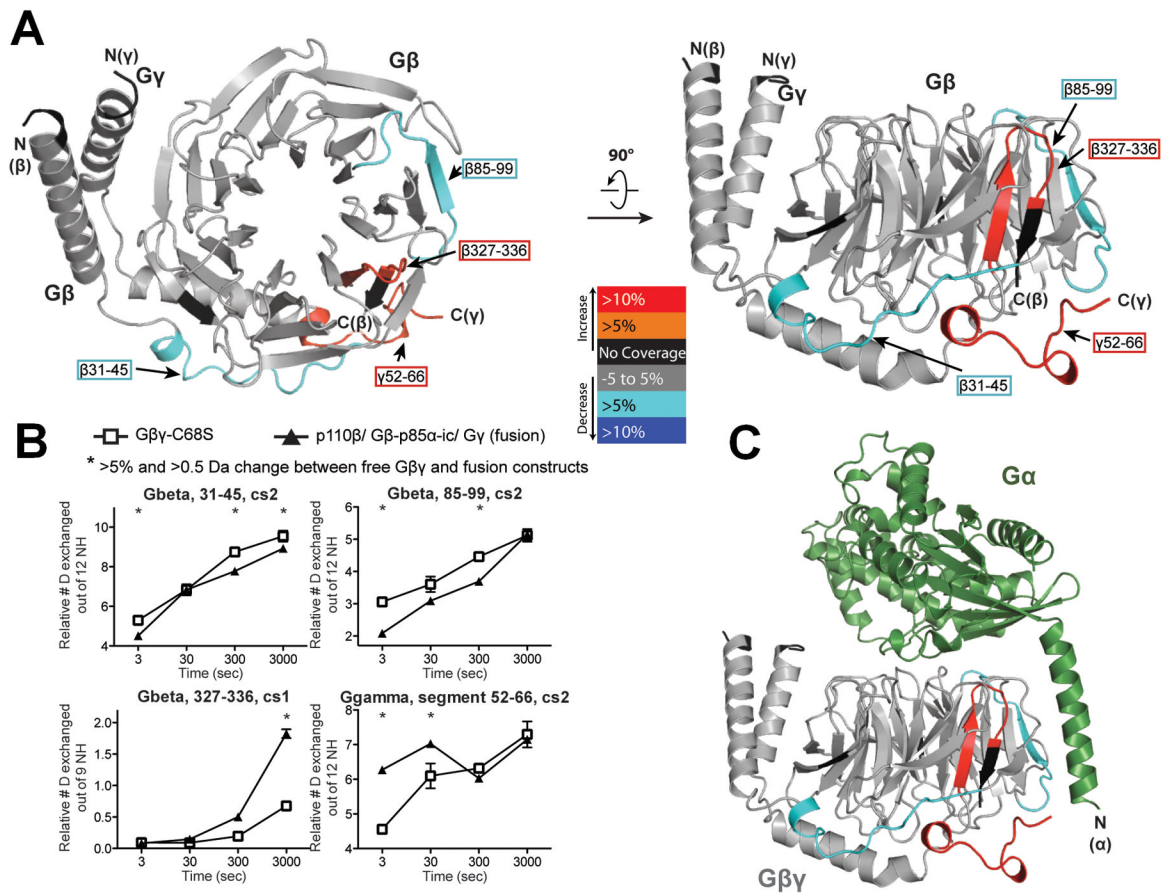


Fig. 2. Role of $G\beta\gamma$ in PI3K β -mediated signaling, transformation, motility, and invasion. **(A)** HEK 293E cells were transfected with plasmids encoding myc-Akt and either WT or the ^{532}KK -DD mutant PI3K β , with or without plasmids encoding $G\beta\gamma$. Akt activation in samples immunoprecipitated (IP) with an antibody against myc was analyzed by Western blotting with an antibody against pT308-Akt. The ratio of the amount of pAkt to that of total Akt is expressed as a percentage of that under basal conditions. **(B)** NIH3T3 cells stably expressing WT or mutant PI3K β were stimulated with 10 nM LPA for 5 min. Akt activation was analyzed by Western blotting with anti-pT308-Akt antibody and quantified as described earlier. **(C)** HEK 293T cells were transfected with plasmid encoding WT or ^{532}KK -DD mutant p110 β . Cell lysates were incubated with GST or GST-Rab5 immobilized on glutathione-Sepharose beads, and bound material was analyzed by Western blotting. Graphs in each panel show the mean percentage pull-down \pm SEM from three separate experiments. **(D and E)** NIH3T3 cells were transfected with plasmids encoding p85 α and either WT or the ^{532}KK -DD mutant p110 β , and **(D)** the formation of colonies in soft agar or **(E)** the formation of foci were measured. Graphs in each panel show means \pm SEM from three separate experiments. **(F)** Migration of control NIH3T3 cells or cells stably expressing WT or mutant PI3K β towards FBS was measured in a Boyden chamber assay. Assays were conducted in triplicate, and the data are pooled from two separate experiments.

**Fig. 3.**

Mapping of the p110 β -binding region in G $\beta\gamma$ heterodimers with HDX-MS. (A) The p110 β -G β -p85 α -icSH2-G γ -C68S fusion heterotrimer (fusion) was used to compare deuterium incorporation with that of free G $\beta\gamma$ -C68S (G $\beta\gamma$). Regions in G β and G γ that showed >0.5 Dalton and >5% changes between free G $\beta\gamma$ and the fusion were mapped onto the G $\beta\gamma$ model (PDB ID: 1GOT). In addition to the protected peptides described in the text, there was some exposure of the C-terminus of G β and the adjacent C-terminus of G γ , which were probably a consequence of the attachment of the C-terminus of G β to the linker connecting to p85 in the fusion. (B) All peptides in G β and G γ that showed changes in deuteriation extent between free G $\beta\gamma$ and the fusion proteins are shown. The stretch of amino acid residues 52 to 66 in G γ is labeled as a segment to denote that these data were generated by subtraction of the deuterium incorporation of peptide 44 to 51 from that of peptide 44 to 66. * indicates changes that were >0.5 Dalton and >5%. Experiments were performed in duplicate and graphs show the SD. (C) Crystal structure of G $\beta\gamma$ bound to G α (PDB ID: 1GOT). G $\beta\gamma$ is colored as in (A).

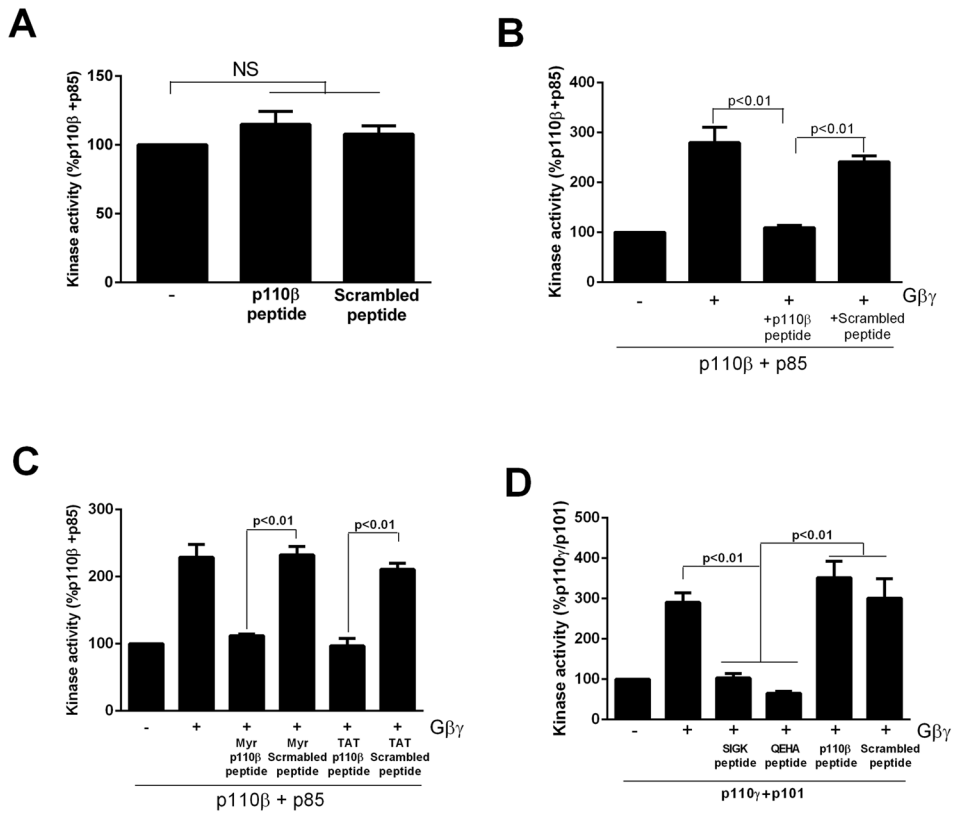


Fig. 4. A peptide derived from p110β blocks the activation of PI3Kβ by G βγ in vitro. **(A)** PI3Kβ immunopurified from HEK 293T cells was incubated in the absence or presence of 1 μM p110β-peptide or scrambled peptide and assayed for lipid kinase activity. **(B)** PI3Kβ immunopurified from HEK 293T cells was incubated in the absence or presence of recombinant lipidated Gβγ and 1 μM p110β-peptide or scrambled peptide and assayed for lipid kinase activity. **(C)** PI3Kβ immunopurified from HEK 293T cells was incubated in the absence or presence of recombinant lipidated Gβγ and 1 μM myristoylated or TAT-tagged p110β-peptide or scrambled peptide and assayed for lipid kinase activity. **(D)** Immunopurified p101–p110γ from HEK 293T cells was incubated with or without recombinant lipidated Gβγ and 1 μM p110β-peptide, scrambled peptide, 1 μM QEHA peptide, or 10 μM SIGK peptide. Data in all panels are the means ± SEM of triplicate measurements and are representative of two to three experiments.

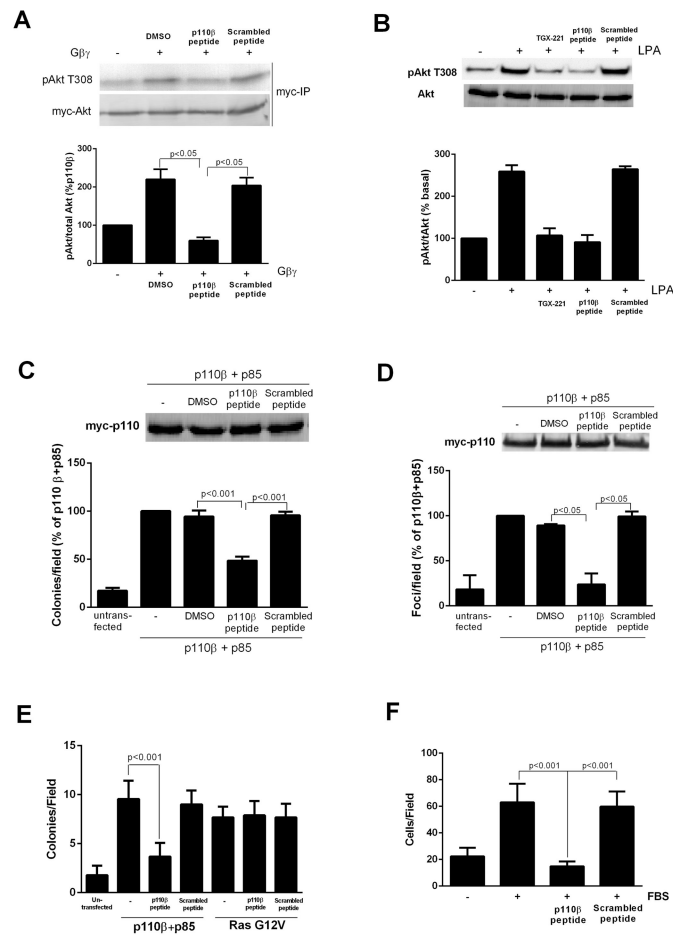


Fig. 5. Peptide inhibitors disrupt PI3K β activation and signaling in response to G $\beta\gamma$. **(A)** HEK 293E cells were transfected with plasmids encoding p110 β , p85, and myc-Akt with or without plasmid encoding G $\beta\gamma$. Cells were treated with 30 μ M peptide or scrambled peptide for 30 min, and the extent of phosphorylation of Akt at Thr³⁰⁸ (T308) was determined by Western blotting analysis. **(B)** NIH3T3 cells were pretreated with TGX221, p110 β -peptide, or scrambled peptide and stimulated with 10 nM LPA for 5 min before the extent of phosphorylation of Akt at Thr³⁰⁸ was determined by Western blotting analysis. **(C)** NIH3T3 cells were transfected with plasmids encoding WT p110 β and p85 α , and colony formation in soft agar was measured in the absence or presence of 30 μ M p110 β -derived myristoylated peptide or scrambled peptide. **(D)** NIH3T3 cells were transfected with plasmids encoding WT p110 β and p85 α , and foci formation was measured in the absence or presence of 30 μ M p110 β -derived myristoylated peptide or scrambled peptide. **(E)** NIH3T3 cells were transfected with plasmids encoding p110 β and p85, or with plasmid encoding ¹²V-Ras. Cells were incubated with or without p110 β -peptide or scrambled peptide, and formation of colonies in soft agar was measured. **(F)** Migration of NIH3T3 stably expressing p110 β and p85 α towards FBS in a Boyden chamber, in the absence or presence of p110 β -peptide or scrambled peptide. The graphs in each panel show means \pm SEM from three to four separate experiments. Data in (E) show means \pm SEM from triplicate measurements and are representative of two experiments.

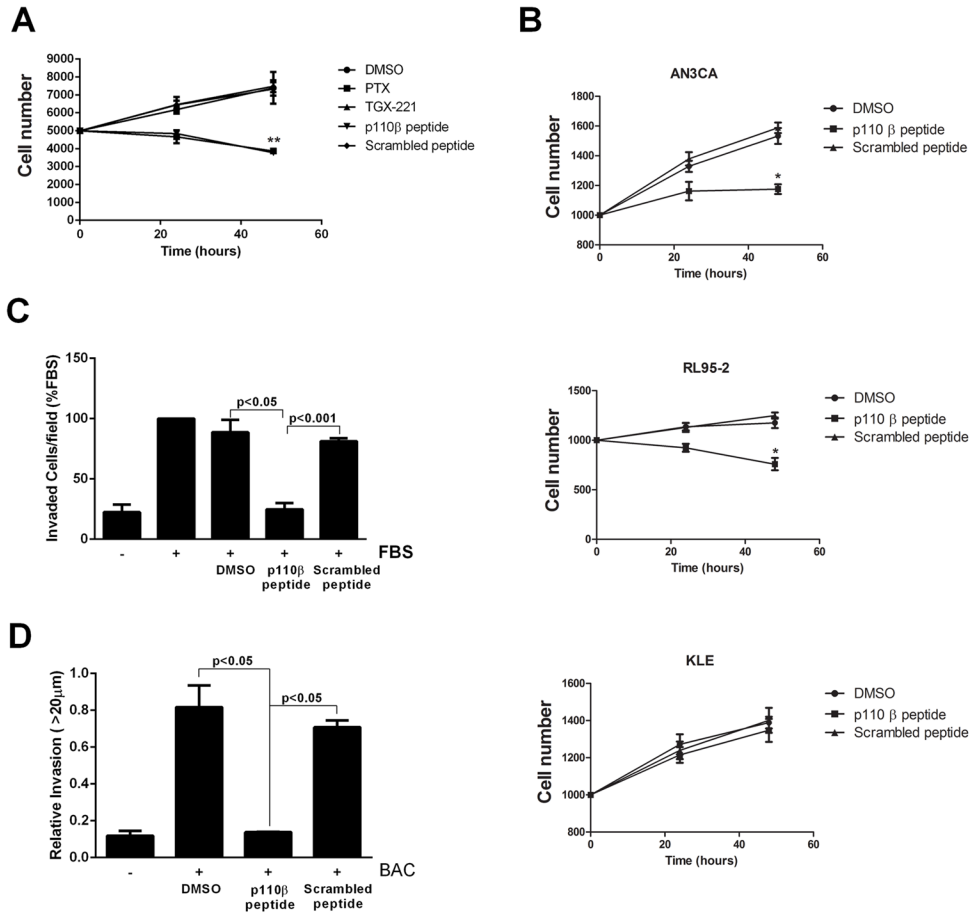


Fig. 6. Inhibition of the proliferation and chemotaxis of prostate cancer cells. **(A)** Proliferation of PC-3 cells was measured by the MTT assay in the absence or presence of 200 nM TGX221, 30 μM myristoylated p110β-derived peptide, or 30 μM scrambled peptide. **(B)** Proliferation assays were performed on two PTEN-null endometrial cancer cell lines (AN3CA and RL95-2 cells) and one PTEN-positive endometrial cancer cell line (KLE cells) grown in the absence or presence of myristoylated p110β-derived peptide or scrambled peptide. **(C)** Chemotaxis of PC-3 cells towards 10% FBS in the absence or presence of 20 μM p110β-derived peptide or scrambled peptide was measured in Boyden chambers. **(D)** Bone marrow-derived macrophages and Cell-tracker-red-labeled PC-3 tumor cells were co-plated in 24-well dishes and overlaid with collagen. Cells were incubated for 24 hours in the absence or presence of p110β-derived peptide or scrambled peptide, and invasion into the collagen was measured by confocal microscopy. The data are means ± SD from two separate experiments for (B) and (D), and are means ± SEM from three separate experiments for (A) and (C).